Available online at www.sciencedirect.com

SCIENCE DIRECT®

Polymer 47 (2006) 1487–1495

polymer

www.elsevier.com/locate/polymer

# Small-angle X-ray scattering and linear melt rheology of poly(*tert*-butyl acrylate-*g*-styrene) graft copolymers

J.L. de la Fuente [a,*], M. Fernández-García [b], M.L. Cerrada [b], H.W. Spiess [c], M. Wilhelm [c,d]

[a] *Instituto Nacional de Técnica Aeroespacial 'Esteban Terradas', INTA, Crta. de Ajalvir, Km 4. 28850 Torrejón de Ardoz, Madrid, Spain*
[b] *Instituto de Ciencia y Tecnología de Polímeros (CSIC), Juan de la Cierva, 3. 28006 Madrid, Spain*
[c] *Max-Planck Institut für Polymerforschung, Ackermannweg 10, 55128 Mainz, Germany*
[d] *Fachbereich Mechanik, TU-Darmstadt, 64289 Darmstadt, Germany*

Received 4 October 2005; received in revised form 22 December 2005; accepted 13 January 2006

## Abstract

The morphology and rheological properties have been studied for poly(*tert*-butyl acrylate-*g*-styrene), P*t*BA-*g*-S, graft copolymers through the analysis of different samples that varied in the number of grafted repeat units. Small-angle X-ray scattering (SAXS) measurements confirmed phase separation in these samples, and showed the presence of disordered microdomains on those copolymers with a grafting number higher than 7. SAXS results have also shown a significant improvement of microdomain segregation with temperature manifesting considerable changes in both intensity, position and full-width half-maximum of the peak $q^*$, which is attributed to the graft-like nature of these systems. The frequency dependence of the dynamic moduli revealed three relaxation mechanisms. The low-frequency (long time) relaxation was identified with the movement of the whole molecule, the relaxation at intermediate time is related to movement of the grafts, and the high-frequency relaxation is like that found in the transition zone of main chain of poly(*tert*-butyl acrylate), P*t*BA. The rheological measurements indicated that the introduction of a small amount of polystyrene, PS, grafts in the P*t*BA backbone is sufficient to modify mechanical behaviour at low frequencies. Comparison of the rheological properties of the graft copolymers with higher PS content showed that the observed changes in the viscoelastic behaviour under shear seems to be related to both the microphase separated microstructure and the number of grafts present in the copolymers.

*Keywords:* Poly(*tert*-butyl acrylate-*g*-styrene) graft copolymers; SAXS; Rheological properties

## 1. Introduction

Block copolymers are versatile in displaying a wide assortment of possible compositions, architecture and monomers, which lead to dramatic changes in self-assembly at the mesoscale level and, consequently, in physical properties [1]. One of the most striking features of this type of macromolecule is that, in the molten state, the different chemical units might separate into microphases at low temperatures to form ordered microdomains. Although block copolymers have been the subject of extensive investigation during the past three decades, fewer studies were devoted to the morphology and physical properties of block copolymers with non-linear architectures, such as, i.e. star blocks and graft copolymers [2].

Grafted molecular architectures, respective topologies, are shown to be an additional factor which affects the morphological behaviour of these block copolymers, in addition to volume fraction and degree of segregation. Although the experimental data for graft copolymers are scarce, theoretical studies have pointed out several features with respect to linear diblock copolymers [3–5]. These studies have shown the different particularities that present these non-linear systems with respect to the corresponding linear diblock copolymers, due to mainly its inherent asymmetry. Moreover, Benoit and Hadziioannou [5] have developed a general theory to predict the scattering profiles in the homogeneous state, and phase separation behaviour of multiblock copolymers analysing various architectures such as linear, graft and star. These two authors described in detail the influence of different fundamental variables on these scattering profiles (such as the radius of gyration of each block, degree of polymerisation, number of sequences, polymolecularity in molecular weight and composition).

On the other hand, the presence of long chain branching has a dramatic effect on dynamical and rheological behaviours in well-entangled polymers. The theory is particularly well-

---

* Corresponding author. Tel./fax: +34 91 5201841.
*E-mail address:* fuentegj@inta.es (J.L. de la Fuente).

0032-3861/$ - see front matter © 2006 Elsevier Ltd. All rights reserved.
doi:10.1016/j.polymer.2006.01.041

developed for the rheology of homopolymers with the simplest branched architecture. Model polymers with well-defined architectures have been crucial in advancing the understanding of polymer melt dynamics. The success of these theories in describing the simplest polymer architectures, such as linear and star polymers, has stimulated further development in the understanding of the dynamics of melts of more complicated architectures, such as star–star [6] and star–linear blends, [7] as well as H-shaped polymers [8]. These investigations motivated the study of comb-shaped polymer melts. Novel and significantly different linear rheological response was found at lower frequencies in comb polymers compared to other branched macromolecular structures [9,10].

However, most experimental and theoretical (being the great relevance the contributions of Larson on the quantitative models [11]) studies reported in the literature focus on homopolymers [12–20]. In contrast, the rheological behaviour has been studied less extensively in block copolymer materials with branched architecture (for example, graft copolymer ($AB_n$), miktoarm star copolymers ($A_nB_m$) and miktoarm star terpolymers (ABC)). Therefore, a whole new dimension in block copolymer research is stimulated by concerning, primarily, the interplay of molecular architecture (topology) and the phase separated morphology on solution and melt properties of these block copolymer systems.

Graft copolymers have long been of interest as a result of the diverse and important technical applications, such as interface compatibilizer in blends. Several studies of these copolymers have been carried out previously, however, many of these works were limited to samples with well-defined architectures, [2a,b] paying less attention to those samples commonly used as blend compatibilizers, which generally present higher polydispersities and/or ill-defined architectures.

The aim of this investigation is to study such block copolymer systems by examining the morphological aspects, and the effect of the grafted architecture on the rheology of a set of graft copolymers. Poly(*tert*-butyl acrylate-*graft*-styrene), P*t*BA-*g*-S, have been synthesized with different grafting densities by free-radical polymerisation using the macromonomer technique [21]. Therefore, all the copolymers have a backbone of poly(*tert*-butyl acrylate), P*t*BA, with a molecular weight of ~150 kg/mol and grafts of polystyrene, PS, of 13 kg/mol molecular weight, where the PS-chains are statistically distributed along the acrylate backbone. The synthesis, thermal properties, solid-state viscoelastic behaviour, and microhardness measurements of these graft copolymers were described in earlier papers [21,22]. The specimens were prepared by compression moulding in order to correlate the viscoelasticity and microhardness with their morphology and rheology response. The published reports on this material indicate a phase separation and, therefore, the existence of microdomains of the two components for a determined degree of grafting. This is the starting point for the X-ray and melt rheology study ($T > T_g$) presented here.

## 2. Experimental

### 2.1. Graft copolymers

The methods used for the synthesis and characterization of these graft copolymers were given in a previous paper [21]. Some of their molecular characteristics, such as the values of the apparent weight-average, number-average molecular weight and number of grafts per chain obtained are listed in Table 1. This table also includes the glass transition temperatures, estimated from dynamic mechanical measurements under bending deformation, for the different samples investigated [22].

### 2.2. Specimen preparation

For rheological and SAXS measurements, the samples P*t*BA, macromonomer PS, and the different graft copolymers were processed by compression moulding in a press between hot plates (disks with 8 mm of diameter and a thickness of 1 mm), at temperatures of 90 °C (P*t*BA) and 120 °C (PS and P*t*BA-*g*-S), at a pressure of 2 MPa for 20 min. Subsequently, they were quenched to room temperature. Additional copolymer films were prepared by casting from a ~5% (w/v) toluene solution. To further promote the formation equilibrium morphologies, the bulk films were annealed under vacuum at 120 °C during 72 h. The films were then cooled slowly to room temperature.

### 2.3. Techniques

Small-angle X-ray scattering, SAXS, measurements were performed employing synchrotron radiation (with $\lambda =$

Table 1
Molecular characteristics and rheological parameters of the P*t*BA-*g*-S copolymers and homopolymer samples, P*t*BA and PS (reference temperature 120 °C)

| Polymer | $\bar{M}_n$ (kg/mol) | $\bar{M}_w$ (kg/mol) | $N_{graft}$ | $T_g$[a] (°C) | $C_1$ | $C_2$ (K) | $G_{N\ \mathrm{1st\ app}}^0$ (Pa) | $G_{N\ \mathrm{2nd\ app}}^0$ (Pa) | $G_{N\ \mathrm{(calcd)}}^0$[b] (Pa) |
|---|---|---|---|---|---|---|---|---|---|
| P*t*BA | 148 | 379 | – | 75 | 6.9 | 140.3 | | $6.4\times10^4$ | |
| P*t*BA-*g*-S1 | 175 | 465 | 7 | 76 | 22.9 | 370.5 | $1.0\times10^5$ | $2.7\times10^4$ | $4.0\times10^4$ |
| P*t*BA-*g*-S2 | 170 | 509 | 10 | 77; 114 | 11.6 | 155.0 | $1.1\times10^5$ | $2.8\times10^4$ | $3.0\times10^4$ |
| P*t*BA-*g*-S3 | 178 | 569 | 15 | 79; 115 | 13.3 | 128.9 | $2.3\times10^5$ | $1.9\times10^4$ | $2.4\times10^4$ |
| P*t*BA-*g*-S4 | 204 | 797 | 32 | 81; 117 | 9.0 | 86.3 | $2.2\times10^5$ | $1.1\times10^4$ | $1.2\times10^4$ |
| PS | 13.0 | 13.6 | – | – | 8.3 | 83.1 | – | – | – |

[a] Estimated by dynamic mechanical measurements (tan $\delta$) under bending deformation [22]. For PS sample could not be determined due to the film fragility.
[b] Calculation of apparent plateau modulus from Eq. (2), assuming backbone is diluted by the grafts and $\alpha = 2.22$.

0.150 nm) in the beamline A2 at HASYLAB (Hamburg, Germany). A linear position-sensitive detector was used at a distance of 235 cm from the sample and calibrated with the different orders of the long spacing of rat-tail cornea ($L=65$ nm). It was found to cover a spacing range from 5 to 55 nm. A heating rate of 10 °C/min was used, acquiring data in time frames of 30 s. More details on the instrumentation can be found in Ref. [23]. The profiles are presented as a function of magnitude of scattering vector $q$, which is given by $q=(4\pi/\lambda)(\sin(\theta/2))$, where $\lambda$ and $\theta$ are the wavelength of X-ray and the scattering angle, respectively. The scattered intensity is shown in a logarithmic scale in arbitrary units.

Rheological testing was performed with an Advanced Rheometric Expansion System (ARES, Rheometrics Scientific) in the oscillatory mode with parallel-plate fixtures (8 mm) and a 2KFRTN1-transducer. Dynamic frequency sweep experiments were conducted to measure the shear storage and loss moduli ($G'$ and $G''$) as a function of angular frequency ($\omega$) ranging from 0.1 to 100 rad/s at various temperatures (the highest temperature used did not exceed 180 °C). Master curves were constructed from the isothermal measurements in frequency sweeps using time–temperature superposition. Frequency sweeps required to maintain a constant gap between the plates (sample thickness) to compensate for tooling expansion/contraction. The strain amplitude applied to each specimen was chosen to ensure that the obtained data were within the linear viscoelastic regime. All measurements were conducted under a nitrogen atmosphere in order to avoid oxidative degradation of the samples. Moreover, it was necessary to ensure that no significant degradation of the samples occurred at high temperatures. The initial frequency test was always performed at 140 °C, and after testing at the highest temperatures for a particular specimen, the measurement was repeated again at 140 °C. In general, a very good agreement was observed between the two 140 °C measurements (initial and final one). The only experiment with a strain amplitude corresponding to the non-linear viscoelastic range was performed to induce orientational order in the material with large amplitude oscillation ($T=130$ °C, $\omega=1$ rad/s, and the strain amplitude $\gamma_0=0.3$). The sample was subsequently quenched to ambient temperature and examined by SAXS.

## 3. Results and discussion

### 3.1. SAXS measurements

The microdomain morphology of block copolymer systems depends not only on the relative volume fraction of the constituents, but also on the processing conditions and thermal history. It is generally recognised that the entire spectrum of properties is closely related to the microdomain morphology developed in the specimens. Therefore, knowledge of the morphological details of a given specimen is of special interest [24,25]. Our previous investigations concerning P*t*BA-*g*-S graft copolymers showed the existence of phase segregation in the compressed-moulded specimens when the number of PS grafts per backbone chain was in the order of 10 or higher.

Fig. 1 shows the corresponding SAXS profiles for P*t*BA-*g*-S2 and P*t*BA-*g*-S4 in a heating experiment. The analysis of the different profiles as a function of temperature allows information to be obtained about the morphological variation during increasing temperature in these samples. The copolymer with the lowest PS grafted content, P*t*BA-*g*-S1, does not exhibit any Bragg peak, thus confirming our previous DSC and DMTA results on the non-existence of microdomains segregation [21,22]. On the contrary, P*t*BA-*g*-S2 specimen shows a weak and broad shoulder at room temperature that is much better defined, increasing its intensity and moving to higher $q^*$ values as the temperature is raised. As the graft density increases, e.g. in P*t*BA-*g*-S4 profiles, $q^*$ is shifted to higher values and, consequently, spacing is reduced because the backbone block between grafts becomes smaller. The lack of higher order reflections points out the presence of not arranged microdomains in these samples under the current experimental conditions used.

The variation of the relative invariant [26] calculated from the SAXS data in the heating process gives an idea of the macroscopic electron density fluctuations. The upper plot of

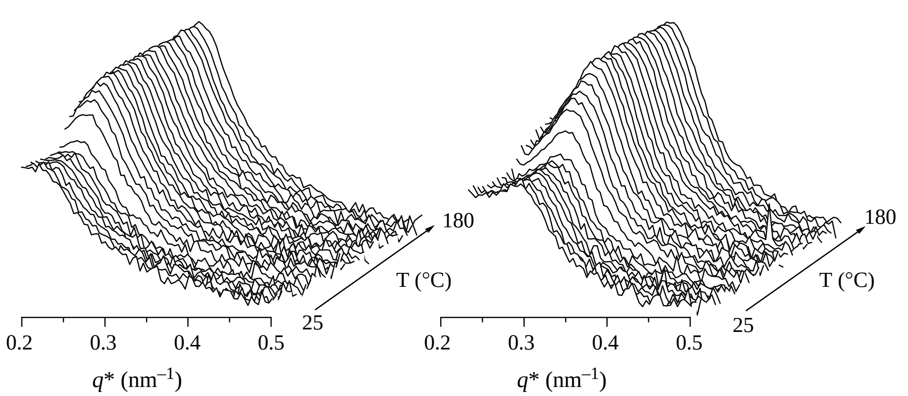

Fig. 1. Real-time SAXS profiles, obtained with synchrotron radiation for P*t*BA-*g*-S2 and P*t*BA-*g*-S4 in a heating experiment from 25 to 180 °C at 10 °C/min. Lines are drawn every 5 °C.

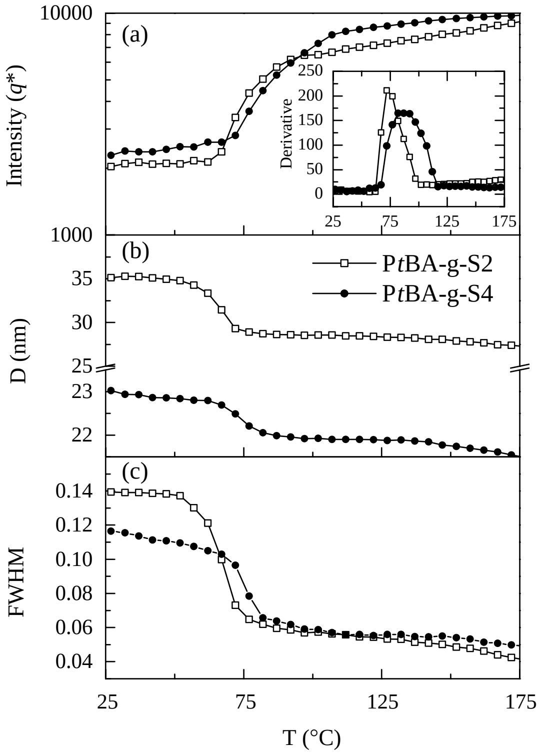

Fig. 2. (a) Relative SAXS $q^*$ intensity of P*t*BA-*g*-S2 and P*t*BA-*g*-S4 and its derivative (inset) during the heating experiments. (b) Variation of periodicity and (c) full-width half-maximum (FWHM) with the temperature for P*t*BA-*g*-S2 and P*t*BA-*g*-S4.

Fig. 2 depicts different fluctuation regions from the intensity changes. At low temperature up to around 80 °C, the first one is related to microdomain arrangements caused after compression moulding and quenching. Interestingly, a clear increase of the $q^*$ intensity occurs at the beginning of this region, indicating that important microdomain reorganization processes are involved as the copolymer attains higher mobility close to the glass transition of the rigid PS grafts. The second fluctuation region is associated with these new backbone/graft arrangements. The development of this ordering is clearly observed in the derivative of the SAXS invariant shown as an inset of the upper plot in Fig. 2. This ordering is dependent on the number of grafts occurring at lower temperature, and in a narrow temperature range as mobility of these copolymeric systems is reduced. At the same temperature region, spacing and width significantly decrease, indicating a morphology densification and narrowness of diffractions, respectively, as seen in the middle and bottom plots in Fig. 2. These features are more pronounced in P*t*BA-*g*-S2 than in P*t*BA-*g*-S4, probably because of initial stronger phase segregation in the latter specimen. P*t*BA-*g*-S3 undergoes an intermediate behaviour.

In order to gain a detailed insight on absence of an ordered regular morphology for these P*t*BA-*g*-S copolymers, additional experiments were carried out on copolymer samples prepared from casting with toluene and further long annealing processes and from large-amplitude oscillation shear (LAOS) experiments [1,27]. However, these SAXS results do not show any sign of a higher order reflections. Exclusively, a light more intense and narrower peak can be observed. These results lead to think that the cause of the poorly organized mesophases in the current copolymers cannot be attributed to kinetic limitations of the imposed processing conditions. Consequently, the inherent architectural asymmetry has a relevant role in the morphological behaviour of these graft copolymers.

In accordance with experimental literature data, the morphologies of microphase-separated non-linear block copolymer, i.e. graft and star, and even blends of diblock copolymers with homopolymers are dominated in part by either wormlike micelles and spheres or by cylinders but not ordered on a lattice [2,28–33]. Also, more chaotic morpholologies along with disordered bicontinuous structures, and even small grain-like regions of more or less coherent domain orientation were found.

### 3.2. Rheology

#### 3.2.1. Linear rheology and time temperature superposition

The linear melt rheology of P*t*BA-*g*-S copolymers must be compared to the different viscoelastic properties exhibited in both ‘parent’ homopolymers: P*t*BA backbone and PS grafts. The comparison of both viscoelastic spectra (copolymers and the corresponding homopolymers) can be used to estimate the influence of the PS grafts on the rheological behaviour of such copolymers. The long time dynamics of linear homopolymer melts are dominated by entanglements and are typically characterized by relaxation spectra that are separated into distinct regions. The high frequency or transition region is associated with local polymer chain motions, and in consequence is independent of molar mass but directly related to the glass transition $T_g$ of the polymer. In contrast, the low frequency, or terminal region is associated with large-scale rearrangements of chain conformations, and becomes increasingly separated from the transition region with augmenting polymer molar mass. The intermediate plateau region is characterized by the plateau modulus, $G_N^0$, which is independent of molar mass. The magnitude of $G_N^0$ reflects the physical structure of the polymer chains and depends on the chain molar mass between entanglements [34].

The rheological characterisation was performed through the construction of master curves, obtained by time–temperature superposition of the isothermal dynamic frequency sweep data in a temperature range from 60 to 180 °C. Excellent superposition of both shear storage modulus, $G'$, and shear loss modulus, $G''$, was observed in essentially all linear homopolymers, P*t*BA and PS. For the graft copolymers good superposition of $G'$ was generally obtained, but a slight dispersion was observed for $G''$. The horizontal shift factors, $a_T$, used to superimpose the curves and validate time–temperature superposition at temperatures from 60 to 180 °C were found to fit the WLF equation well for the different specimens [35]. The $a_T$ values and the best fit WLF curves are shown in Fig. 3, and the parameters $C_1$ and $C_2$ are listed in Table 1. From this figure we note that the temperature dependence of $a_T$ is intermediate between P*t*BA and PS for temperatures below the reference temperature, 120 °C, while a

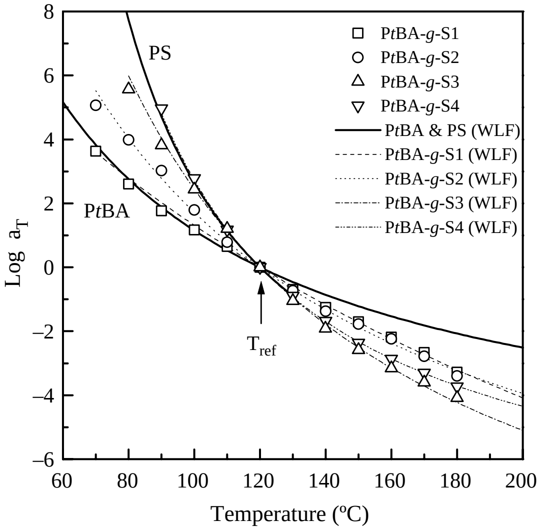

Fig. 3. Linear-log plot of horizontal shift factors $a_T$ as a function of temperature and best fit WLF curves for P*t*BA-*g*-S copolymers. The WLF curves for P*t*BA and PS homopolymers are also plotted as reference.

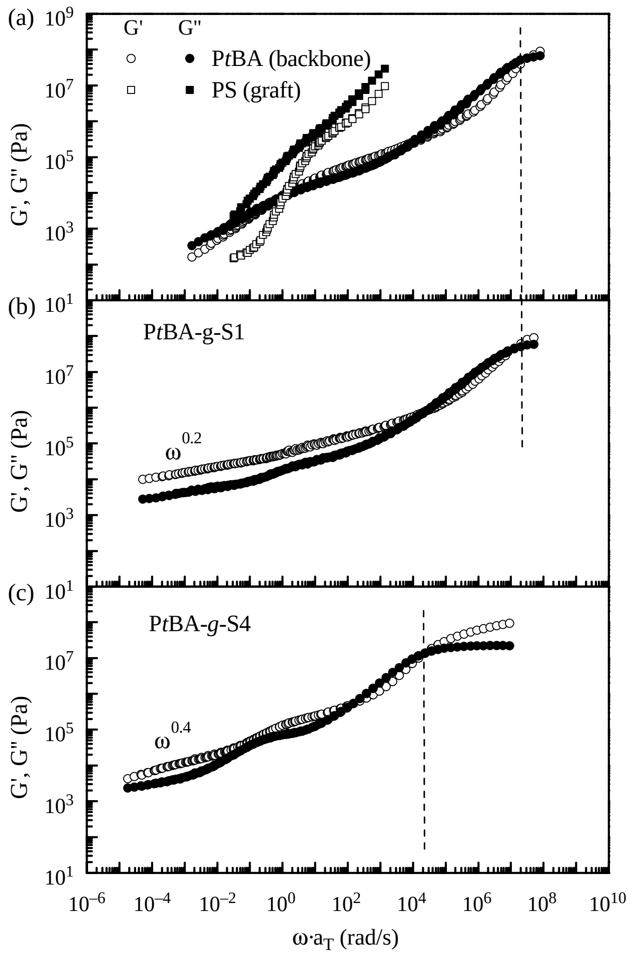

Fig. 4. Dynamic moduli-frequency master curves, storage ($G'$, open symbols) and loss ($G''$ solid symbols), for homopolymers (P*t*BA and PS) and copolymers (P*t*BA-*g*-S1 and P*t*BA-*g*-S4). Reference temperature is 120 °C. Vertical lines indicate the crossover frequency from segmental to Rouse-like dynamic (see text).

different behaviour, not that of pure P*t*BA, is found for higher temperatures. This feature suggests that the existence of microdomains has influenced the rheological behaviour and at the same time there is an additional indication that the segregation between both blocks is not very strong, so that there should be a substantial amount of P*t*BA chain even within the PS rich domain and vice versa.

The upper plot in Fig. 4 shows the master curves $G'$ and $G''$ for the parent homopolymers (P*t*BA and PS) at the reference temperature of 120 °C. The curves for P*t*BA clearly show the usual different regions (transition where $G'' > G'$, rubbery plateau where $G' > G''$ and terminal region where $G'' > G'$) expected for entangled linear homopolymers. On the other hand, the viscoelastic behaviour for PS is typical of polymer melts of low molecular weight, since $M_n$ is lower than the average molecular weight of chain entanglement, $M_e$, which is around 17 kg/mol [35]. Consequently, PS presents a viscous-like behaviour because of the non-existence of entanglements, and the loss modulus exceeds the storage modulus in the entire frequency range.

The studies of the rheological behaviour of polyacrylates are uncommon [36,37], therefore, a detailed analysis of P*t*BA data was conducted. Several relevant characteristics can be seen in the P*t*BA curves, especially in the rubbery and terminal zones. One of the most important parameters in the rubbery zone is the pseudo-equilibrium modulus of the entanglement network, which can be related to the $M_e$ through the equation

$$G_N^0 = \rho RT/M_e \tag{1}$$

where $\rho$ is the polymer density, $R$ is the gas constant and $T$ is the absolute temperature. $G_N^0$ may be calculated from the area under the peak in the loss modulus. However, when this peak is not clearly observed, $G_N^0$ can be alternatively calculated from the $G'$ at the frequency where $\tan\delta$ is at its minimum in the plateau zone. The $G_N^0$ value estimated for the P*t*BA sample was $6.4 \times 10^4$ Pa. The use of $G_N^0$ to calculate $M_e$ provides a means of estimating the minimum molar mass at which entanglements occur. In this case the $M_e$ value calculated from Eq. (1) is 45 kg/mol, which is within the wide variety of published data for other polyacrylates (i.e. poly(*n*-butyl acrylate)), $13 < M_e < 65$ kg/mol [36].

On the other hand, the crosspoint of $G'$ and $G''$ provides information about the elastic and viscous nature of the melt. At the low frequency end of the entanglement plateau, a frequency $\omega_x/2\pi$ is defined by the crosspoint of the master curves of storage and loss moduli, i.e. $G'(\omega_x) = G''(\omega_x)$. At this frequency, the moduli have a value of $6.2 \times 10^3$ Pa.

The lower plots, Fig. 4(b) and (c), depict the master curves for the same two magnitudes, $G'$ and $G''$, in the graft copolymers with the lowest and highest graft content, P*t*BA-*g*-S1 and P*t*BA-*g*-S4, respectively, at a reference temperature of 120 °C. The samples P*t*BA-*g*-S2 and P*t*BA-*g*-S3, showed an intermediate rheological behaviour between the ones presented in this figure. The entire range of viscoelastic behaviour is not observed in these data, since the terminal region was inaccessible for all of the samples due to the phase separation. From these plots, the typical rheological 'signatures' can be observed which are expected from entangled comb-shaped structures [9,10], where different types of entanglements can operate, such as backbone–backbone, backbone–graft and graft–graft entanglements.

Considerable differences can be observed by comparison of linear viscoelastic spectra of the graft copolymers with the ungrafted polymer, P*t*BA, if the same reference temperature is applied. Starting with the response at high frequencies, the sample P*t*BA-*g*-S1 presents a transition region practically identical to that observed in P*t*BA (nearly the same crossover frequency to glass). Contrary to these two samples, the copolymer with more grafts, P*t*BA-*g*-S4, clearly exhibits a different behaviour. The segmental dynamics is slower by nearly 2.5 decades, as demonstrated by the shift of the crossover frequencies from segmental to Rouse-like dynamics in Fig. 4. At the same time, the shear modulus at the transition zone is reduced. This is attributed to the much higher fraction of non-entangled glassy polystyrene compared with that in the other samples, which slows down the overall dynamics of the graft copolymer. Another feature of this sample is that the corresponding modulus at the crossover frequency to the glassy state is lower than those normally observed in a homopolymer, i.e. P*t*BA, and/or the sample P*t*BA-*g*-S1.

More significant changes are observed at lower frequencies in the range of the entanglement plateau. A small amount of PS chains in sample P*t*BA-*g*-S1, is sufficient to broaden the entanglement plateau in the direction of lower frequencies, covering about eight decades. The increase in depth and broadening of the entanglement plateau could be a primary feature of the rheological behaviour of graft copolymers, and should be a result of the interfaces. The dynamic moduli frequency curves of the graft copolymers show two inflexions in the plateau region, indicating the direction of two relaxation processes. Therefore, this broad rubbery plateau is characterised by two regimes. Both $G_N^0$ values were calculated from the $G'$ curves at the frequencies at which tan $\delta$ shows a minimum (see below). A primary apparent plateau at higher frequencies ($G_N^0$ 1st app., see Table 1) is due to the relaxations of the grafts. It is better defined as the number of PS grafts on the main chain increases, and is particularly obvious in the shape of $G''$ curves. This assignment is in agreement with Roovers and Toporoswski [18] who postulate that the reptation of the backbone is conditioned by a previous mechanism of relaxation of the grafts. In this case though, the grafts are so small that they form no entanglements, but act as a diluent and additionally as a structural unit that generates interfaces. The relaxation of the PS chains may be sufficient to limit the relaxation of the backbone. Then, the relaxation of the backbone is possible by constraint release, a process in which the polymer segments can move whenever their entanglements are temporally abandoned. This process has been proposed in the literature [18].

At low frequencies, the onset of a secondary apparent plateau appears ($G_N^0$ 2nd app., see Table 1) when the grafts are completely relaxed. This is attributed to the relaxations of the backbone (i.e. all the segments of the graft copolymer between two graft points). The proposed relaxation of the effective backbone occurs by release of constraints, these restrictions being mostly of the backbone–graft type. Elastic modulus curves at this frequency range do not behave in the same manner as at higher frequencies ($G_N^0$ 1st app. is enhanced when the number of PS chain on the main chain increases). The graft copolymers show not only a smaller apparent plateau as the graft density increases, but also a smaller normal plateau of the linear polymer. The decrease of values of $G_N^0$ means that the backbone in the graft copolymer is far less entangled as the number of PS grafts increases. The value of this apparent plateau modulus can be calculated by assuming that the grafts act simply as a diluent for the backbones, and so it is possible to estimate it from the following equation

$$G_N^0(\phi) = G_N^0(\phi = 1)\phi^{\alpha} \tag{2}$$

where the exponent $\alpha$ has a value between 2.22 [38] and 2.0 [39]. From Table 1 it can be seen that using a value of $6.4\times 10^4$ Pa for $G_N^0(\phi = 1)$ (the plateau modulus for the backbone, P*t*BA, as shown in the same table) and $\alpha = 2.22$ gives quite a reasonable agreement with the data measured for these copolymers.

At the same time, the increase of PS grafts apparently reduces the width of the second plateau. This seems to indicate that the longest relaxation time (accessible experimentally) may depend on the number of grafts. The large graft spacing in P*t*BA-*g*-S1 compared to the P*t*BA-*g*-S4 may provide greater possibility for local cooperation between backbone and grafts. This can be clearly seen in the $G'$ curves of P*t*BA-*g*-S4 sample at the crossover from the entanglement plateau to terminal behaviour, although the frequency $\omega_x$ is not experimentally accessible ($\omega_x$ is approximately the inverse single chain relaxation time in the disordered state) [40].

These findings suggest that the dominant mechanism of relaxation in these copolymers is the graft relaxation (this is more evident for the copolymer with a larger number of grafts). This type of behaviour is characteristic of a variety of macromolecular systems with a large total molecular weight relaxing via branches or segments, generally with small molecular weight below $M_e$. Examples include various non-linear branched polymers [2c], such as dumbbell copolymers [41], super-H-shaped block copolymers [42], etc. Moreover, other polymeric systems, such as that formed by block copolymer micelles in a homopolymer matrix present also three modes of relaxations, similarity to our system under studied [43].

However, it is important to take into account that the dynamics of a graft copolymer is much more complex than in a graft homopolymer. Its rheological behaviour is conditioned by two factors. On one hand, the macromolecular architecture (the number of grafts distributed along the backbone) affects the topology and, on the other hand, the topology leads to the existence of ordered mesophases. The morphology leads to a strong non-linear response. Besides, topological defects present in imperfectly ordered and/or disordered mesophases also affect linear rheological properties. In view of these considerations, it is important to note that in the samples where structural microdomains are better developed (where the polystyrene represents a large fraction, mainly in P*t*BA-*g*-S4, according to SAXS measurements), the slopes of $G'$ in the zone of the secondary apparent plateau takes a value close to 0.4. However, this slope takes a value around 0.2 in that sample where microphase separation is not observed, P*t*BA-*g*-S1. These changes in the scaling exponent in the second apparent plateau can also be related by an alteration in the backbone relaxation mechanisms of the P*t*BA-*g*-4 sample caused by the presence of many graft points, as was mentioned before [17].

### *3.2.2. Application of Cox–Merz rule*

At the lowest frequencies, P*t*BA exhibits a viscous-like behaviour. The viscoelastic properties in this terminal zone are dominated by different parameters that were calculated from Briedis and Faitel'son equation which is equivalent to the Cross model [44]. Actually, this is a particular case of Carreau–Yasuda equation [45] but uses a special case of the Cox–Merz rule where the dynamic viscosity $\eta'(\omega)$ is analysed instead of the steady-state viscosity function $\eta(\dot{\gamma})$ or the absolute value of the complex module $|\eta^*|$.

$$\eta'(\omega) = \eta_0/[1+(\tau_0\omega)^{\alpha}] \qquad (3)$$

where $\eta_0$ the Newtonian viscosity, $\eta_0 = \lim_{\omega\to 0}\eta'$. $\tau_0$ is a relaxation time which inversely accounts for the onset of non-linear pseudoplastic region, and $\alpha$ is a pseudoplasticity or shear thinning index in the range of 0–1. The estimations of these parameters for the P*t*BA sample gave the following values: $\eta_0 = 5.9\times10^5$ Pa s, $\tau_0 = 1.6\times10^3$ s and $\alpha = 0.58$. An additional rheological parameter of the terminal zone is the steady-state compliance, $J_e^0$, defined by its calculation according to the equation

$$J_e^0 = (1/\eta_0^2)\lim_{\omega\to 0}(G'/\omega^2) \qquad (4)$$

This parameter was obtained by extrapolation of the master curves of $G'$ and $G''$, giving a value of $1.04\times10^{-4}$ Pa$^{-1}$.

Another remarkable viscoelastic feature that characterises these polymeric materials is that the melt viscosity is usually higher than that of linear polymers of a similar molecular weight, as is well established in the literature, $(\eta_0)_{\text{comb}} > (\eta_0)_{\text{lin}}$. Thus, for example, Graessley et al. [15–17] observed on model branched star and comb materials (polystyrene and polyisoprene) lower Newtonian viscosities in comparison with linear polymers at the same molecular weight, but an enhancement if these values were compared at a constant radius of gyration. On the other hand, the studies of Long et al. [12] (poly(vinyl acetates)) and Kraus and Gruver [13,14] (polybutadienes) on comb polymers showed that the melt viscosity of these materials was usually higher than that of linear polymers of the same average molecular weight. Similarly, it has been noted for conventional slightly long-chain-branched polyethylenes that the viscosity at low shear rates (in the linear region) may be several times greater than the viscosity of linear polyethylene for the same molecular weight [19,20].

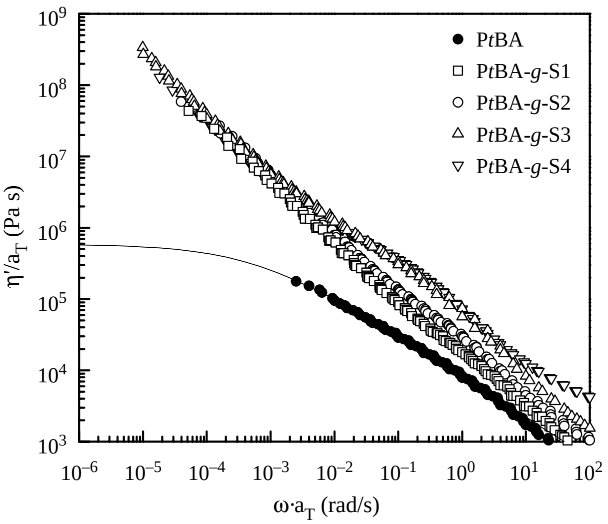

Fig. 5. Comparison of the dynamic viscosity master curves as a function of frequency of P*t*BA-*g*-S copolymer samples and the linear parent P*t*BA (the data are fitted to Eq. (3)). Reference temperature is 120 °C.

The dynamic viscosity master curves are represented in Fig. 5 for the distinct graft copolymers and the P*t*BA homopolymer. The copolymer specimens show a continuous shear thinning region in the frequency range considered, without any indication of levelling off at low frequencies due to the introduction of PS grafts in their architecture. However, in P*t*BA, the levelling off region is observed, since the terminal zone is experimentally reached for this polymer, as seen in its master curve in Fig. 4. Consequently, the value of the parameter $\eta_0$ cannot be associated with the linear (Newtonian) viscosity of the general linear viscoelastic model for the copolymers. However, a clear increase of viscosity (several orders of magnitude) at lower frequencies is observed due to their higher hindrance of reptation introduced by grafts, or the dominantly elastic response due to the large amount of interfaces [46].

### *3.2.3. Van Gurp–Palmen analysis*

To obtain additional information on the influence of molecular architecture on the rheological response of these samples, the so-called Van Gurp–Palmen analysis [47,48] was performed. This method consists of plotting $\delta$ ($=\tan^{-1}[G''/G']$) vs the magnitude of the complex modulus, $|G^*|$ (Fig. 6), and it was used primarily for the characterisation of long chain branching homopolymers, such as polyethylene (giving information about the length and amount of branches) [20]. For linear polymers such as PS, $\delta$ is nearly 90° at low values of $|G^*|$, meaning that the sample response is almost entirely viscous. The point at which the $\delta$ value precipitously drops down (corresponding to complete elastic modulus) is close to the plateau modulus. The behaviour for P*t*BA homopolymer is different from that exhibited by PS. This response can be related to its side chains composed by bulky *tert*-butyl groups, in addition to the polydispersity of the sample. Totally different are the Van Gurp–Palmen curves of the graft copolymers with respect to the P*t*BA homopolymer.

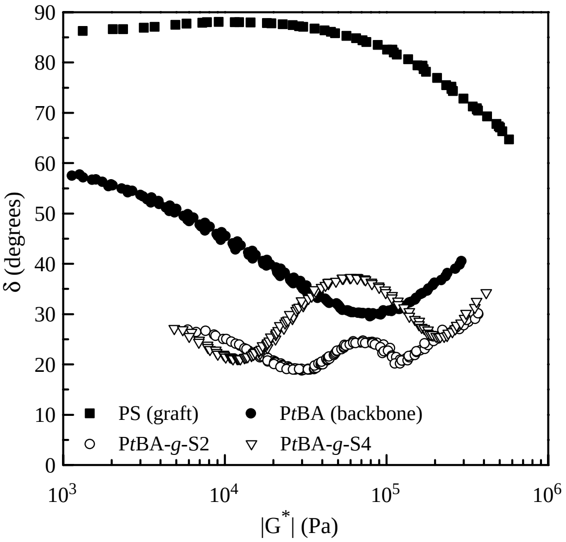

Fig. 6. Van Gurp–Palmen plots for several P*t*BA-*g*-S copolymers. P*t*BA and PS homopolymers data are also plotted for reference.

Note that the minima in $\delta$ are close to the values of the apparent plateaus. This can be used to estimate the secondary plateau modulus for samples, which could not be calculated from the integration of the $G''$ data. Moreover, the differences in the area under the curves are related to the degree of grafting, as shown in this figure.

### *3.2.4. Comparison with linear block copolymer systems*

It is well established that physical characteristics of phase separation in block copolymer systems, i.e. typical triblock copolymers (consisting of outer PS blocks and inner polybutadiene or polyisoprene) persists beyond the upper (PS) glass transition temperature. Their unique thermo-mechanical properties are associated with multi-phase morphology of PS microdomains dispersed in a continuous rubbery matrix, by the hard polystyrene microdomains, and by the slippage of the entangled rubbery chains, which contributes to delay the ductile failure of the PS microdomains. This behaviour is analysed in-depth in the literature [27a,49] for linear block copolymers, and has also been described on a few occasions in graft copolymers. A recent study demonstrated that copolymers containing non-polar hydrocarbons such as polyisoprene in the main chain, and polar functional segments of poly(methyl methacrylate) or PS as side chains show these mechanical properties [33]. The results presented here show that these copolymer systems exhibit a behaviour similar to classical thermoplastic elastomers. PS grafts cause rigid domains connected to a more flexible P*t*BA backbone. Grafts and backbone segregate to form pseudo-two phase aggregates due to thermodynamic differences. In addition, investigation of the response of graft copolymers under linear deformation is essential for the understanding of molecular dynamics in systems much more complicated than graft homopolymers. This complexity is due to occurrence of a phase-separated morphology that strongly affects the linear viscoelastic response, especially at long time/low frequency. Therefore, more studies are needed to elucidate the interplay between single chain behaviour and the dynamics of structural elements within the phase-separated polymer melts.

## Acknowledgements

This research has been supported by the 'Comisión Interministerial de Ciencia y Tecnología', project MAT2004-00496, and the EU-project CAPS (Complex Architecture in Diblock Copolymer Based Polymer Systems), no. FMRX-CT97-0112 (DG 12-DLCL). J.L. de la Fuente acknowledges the hospitality of MPIP in Mainz and partial support for this work from the CAPS EU-project. The synchrotron work (in the A2 polymer line of Hasylab at DESY, Hamburg) was supported by the European Community—Research Infrastructure Action under the FP6 'Structuring the European Research Area' Programme (through the Integrated Infrastructure Initiative 'Integrating Activity on Synchrotron and Free Electron Laser Science') (Contract RII3-CT-2004-506008). We thank the collaboration of the personnel of Hasylab, especially Dr S. Funari.

## References

[1] (a) Hamley IW. The physics of block copolymers. Oxford: Oxford University Press; 1998.
(b) Hadjichristidis N, Pispas S, Floudas G. Block copolymers: synthetic strategies, physical properties, and applications. New York: Wiley; 2003.
(c) Hamley IW. Developments in block copolymer science and technology. New York: Wiley; 2004.
[2] (a) Beyer FL, Gido SP, Buschl C, Iatrou H, Uhrig D, Mays JW, et al. Macromolecules 2000;33:2039.
(b) Xenidou M, Beyer FL, Hadjichristidis N, Gido SP, Tan NB. Macromolecules 1998;31:7659.
(c) Pakula T. Macromol Symp 2004;214:307.
[3] Milner ST. Macromolecules 1994;27:2333.
[4] Olvera de la Cruz M, Sanchez IC. Macromolecules 1986;19:2501.
[5] Benoit H, Hadziioannou G. Macromolecules 1988;21:1449.
[6] Blottiére B, McLeish TCB, Hakiki A, Young RN, Milner ST. Macromolecules 1998;31:9295.
[7] Milner ST, McLeish TCB, Young RN, Hakiki A, Johnson JM. Macromolecules 1998;31:9345.
[8] McLeish TCB, Allgaier J, Bick DK, Bishko G, Biswas P, Blackwell R, et al. Macromolecules 1999;32:6734.
[9] Daniels DR, McLeish TCB, Crosby BJ, Young RN, Fernyhough CM. Macromolecules 2001;34:7025.
[10] Kapnistos M, Vlassopoulos D, Roovers J, Leal LG. Macromolecules 2005;38:7852.
[11] Larson RG. Macromolecules 2001;34:4556.
[12] Long VC, Berry GC, Hobbs LM. Polymer 1964;5:517.
[13] Gruver T, Krauss G. J Polym Sci, Part A-2 1964;2:898.
[14] Krauss G, Gruver T. J Polym Sci, Polym Phys Ed 1965;3:105.
[15] Graessley WW, Roovers J. Macromolecules 1979;12:959.
[16] Raju VR, Rachapudy H, Graessley WW. J Polym Sci, Polym Phys Ed 1979;17:1223.
[17] Roovers J, Graessley WW. Macromolecules 1981;14:766.
[18] Roovers J, Toporowski PM. Macromolecules 1987;20:2300.
[19] Vega JF, Santamaria A, Muñoz-Escalona A, Lafuente P. Macromolecules 1998;31:3639.
[20] Lohse DJ, Milner ST, Fetters LJ, Xenidou M, Hadjichristidis N, Mendelson RA, et al. Macromolecules 2002;35:3066.

[21] Fernández-García M, de la Fuente JL, Cerrada ML, Madruga EL. Polymer 2002;43:3173.

[22] Cerrada ML, de la Fuente JL, Madruga EL, Fernández-García M. Polymer 2002;43:2803.

[23] Elsner G, Riekel C, Zachmann HG. Adv Polym Sci 1985;67:1.

[24] Wang C. Macromolecules 2001;34:9006.

[25] Schmalz H, Böker A, Lange R, Krausch G, Abetz V. Macromolecules 2001;34:8720.

[26] Ryan AJ, Stanford JL, Bras W, Nye TMW. Polymer 1997;38:759.

[27] (a) Bates FS, Fredrickson GH. Annu Rev Phys Chem 1990;41:525.
(b) Fredrickson GH, Bates FS. Annu Rev Mater Sci 1996;26:501.
(c) Wiesner U. Macromol Chem Phys 1997;198:3319.

[28] Beyer FL, Gido SP, Uhrig D, Mays JW, Tan NB, Trevino SF. J Polym Sci, Polym Phys 1999;37:3392.

[29] Ishizu K, Uchida S. Prog Polym Sci 1999;24:1439.

[30] Pochan DJ, Gido SP, Pispas S, Mays JW, Ryan AJ, Fairclough JPA, et al. Macromolecules 1996;29:5091.

[31] Yang L, Gido SP, Mays JW, Pispas S, Hadjichristidis N. Macromolecules 2001;34:4235.

[32] Zhu Y, Weidisch R, Gido SP, Velis G, Hadjichristidis N. Macromolecules 2002;35:5903.

[33] Hong SC, Pakula T, Matyjaszewski K. Macromol Chem Phys 2001;202:3392.

[34] Graessley WW, Edwards SF. Polymer 1981;22:1329.

[35] Ferry JD. Viscoelastic properties of polymer. 3rd ed. New York: Wiley; 1980.

[36] Ahmad NM, Lowell PA, Underwood SM. Polym Int 2001;50:625.

[37] Fetters LJ, Lohse DJ, Graessley WW. J Polym Sci, Part B 1999;37:1023.

[38] Raju VR, Menezes EV, Marin G, Graessley WW, Fetters LJ. Macromolecules 1981;14:1668.

[39] Tao H, Lodge TP, von Meerwall ED. Macromolecules 2000;33:1747.

[40] Zhang Y, Wiesner U. Macromol Chem Phys 1998;199:1771.

[41] Houli S, Iatrou H, Hadjichristidis N, Vlassopoulos D. Macromolecules 2002;35:6592.

[42] Floudas G, Hadjichristidis N, Iatrou H, Avgeropoulos A, Pakula T. Macromolecules 1998;31:6943.

[43] Watanabe H, Sato T, Osaki K, Hamersky MW, Chapman BR, Lodge TP. Macromolecules 1998;31:3740.

[44] Cross MM. J Appl Polym Sci 1969;13:765.

[45] Bird RB, Armstrong RC, Hassager O. Dynamics of polymeric liquids, vol. I. New York: Wiley; 1987.

[46] Langela M, Wiesner U, Spiess HW, Wilhelm M. Macromolecules 2002;35:3198.

[47] Van Gurp M, Palmen J. Rheol Bull 1998;67:5.

[48] Trinkle S, Friedrich C. Rheol Acta 2001;40:322.

[49] (a) Bates FS. Science 1991;251:898.
(b) Legge NR, Holden G, Schroeder HE, editors. Thermoplastic elastomers—a comprehensive review. Munich, Germany: Hansen Publishers; 1998.